EurJOC
European Journal of Organic Chemistry

Research Article
doi.org/10.1002/ejoc.202400298

Chemistry Europe
European Chemical Societies Publishing

www.eurjoc.org

Synthesis and Optical and Theoretical Characterization of Imidazo[5,1-*a*]isoquinolines and Imidazo[1,5-*a*]quinolines

Carina Rössiger,[a, c] Thomas Oel,[a, c] Pascal Schweitzer,[b, c] Olesia Vasylets,[a, c] Michael Kirchner,[a, c] Ajlin Abdullahu,[a, c] Derck Schlettwein,[b, c] and Richard Göttlich*[a, c]

Imidazo[1,5-*a*]quinolines emit intense blue luminescence, suggesting their possible use as emitter molecules in organic light-emitting diodes. We synthesized several new imidazo[5,1-*a*]isoquinolines and found they possessed a characteristic hypsochromic effect and even increased quantum efficiency compared to the homolog imidazo[1,5-*a*]quinolines, as measured by UV-vis- and fluorescence spectroscopy in solution. The energies of the highest occupied and lowest unoccupied molecular orbitals were calculated using density functional theory and experimentally determined by cyclic voltammetry in solution. We obtained a maximum fluorescence quantum yield of 48% at 446 nm for the newly synthesized 3-(4-cyanophenyl)-1-(pyridyl)imidazo[5,1-*a*]isoquinoline with an optimized substitution pattern. For 1-phenyl-3-(2-pyridinyl)imidazo[5,1-*a*]isoquinoline, a quantum yield of 33% was obtained at an even shorter emission wavelength of 431 nm.

Introduction

Organic fluorophores like imidazo[1,5-*a*]pyridines are used in many different medical applications, e.g., as HIV protease inhibitors,[1] thromboxane inhibitors,[2] treatment for estrogen-dependent diseases,[3] heart-strengthening drugs,[4] 5-HT4-receptor antagonists (in the treatment of Parkinson's disease),[5] sedatives,[6] and NSAIDs.[7] Recently, they have been used in other fields[8] like biological cell imaging,[8] as photonic materials, or in organic electronics,[9,10] such as in organic-light-emitting diodes (OLEDs).[11]

Although producing red and green OLEDs is relatively straightforward,[12] blue emission remains a bottleneck in organic optoelectronics. This can be attributed to the short operational lifetimes of blue emitters.[12,13] Therefore, new blue emitter molecules with high quantum yields and high stability are of great interest. Compounds like imidazo[1,5-*a*]pyridines **3**[14] and imidazo[1,5-*a*]quinolines **2** (Figure 1) are also of interest, as they are very stable and show large Stokes shifts.[15]

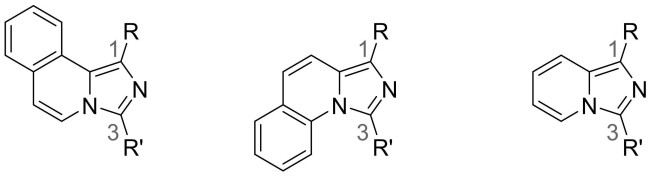

1 **2** **3**

Figure 1. General structure of imidazo[5,1-*a*]isoquinolines **1**, imidazo[1,5-*a*]quinolines **2** and imidazo[1,5-*a*]pyridines **3**.

This property renders re-absorption unlikely and, therefore, suppresses emitter degradation. Winterfield and Franzke described the blue fluorescent properties of imidazo[1,5-*a*]pyridines for the first time in 1963.[16] Reported quantum yields of up to 44% at 485 nm[10] and well-established pathways for their synthesis enhance their potential as OLED materials.[17] The favorable material properties of a particular imidazo[1,5-*a*]quinoline, 1-(pyridine-2-yl)-3-(quinoline-2-yl)imidazo[1,5-*a*]quinoline (PCIC),[18] has led to its use as an emission layer in OLEDs.[9]

Considerable research has already focused on imidazo[1,5-*a*]pyridines[19] and imidazo[1,5-*a*]quinolines with different functional groups, showing the sensitivity of their quantum yield (Φ) and other photo- and electrochemical properties to changes in the π-electron system.[9,19–22]

Zimmer[23] described the synthesis of imidazo[5,1-*a*]isoquinolines **1** in 1968, as did Reimlinger in 1975.[24] Yavari reported a wide range of biological properties of these compounds.[25] Later, Langry[26] and Bori published a convenient synthetic pathway for the preparation of 3-substituted imidazo[5,1-*a*]isoquinolines[27] and 3-substituted imidazo[1,5-*a*]pyridines using selenium dioxide; they also reported on these compounds' blue fluorescence.[28] Pelletier reported the structure of cribostatin-6 (Figure 2). This substance has been isolated from the blue marine sponge Cribochalina sp. and has antibiotic

[a] C. Rössiger, T. Oel, O. Vasylets, M. Kirchner, A. Abdullahu, R. Göttlich
Institute of Organic Chemistry, Justus Liebig University Giessen, Heinrich-Buff-Ring 17, 35392 Giessen, Germany
E-mail: Richard.Goettlich@org.chemie.uni-giessen.de

[b] P. Schweitzer, D. Schlettwein
Institute of Applied Physics, Justus Liebig University Giessen, Heinrich-Buff-Ring 16, 35392 Giessen, Germany

[c] C. Rössiger, T. Oel, P. Schweitzer, O. Vasylets, M. Kirchner, A. Abdullahu, D. Schlettwein, R. Göttlich
Center for Materials Research (ZfM), Justus Liebig University Giessen, Heinrich-Buff-Ring 16, 35392 Giessen, Germany

Supporting information for this article is available on the WWW under https://doi.org/10.1002/ejoc.202400298

Research Article
doi.org/10.1002/ejoc.202400298

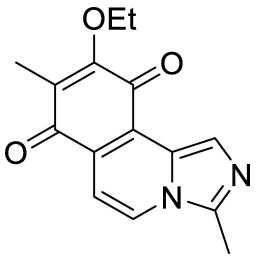

Figure 2. Structure of cribostatin-6, which has been isolated from the blue marine sponge Cribochalina sp.

properties.[29] These examples demonstrate the fascinating and diverse properties of imidazo[5,1-*a*]isoquinolines.

More recently, in 2018, Volpi et al. observed a hypsochromic effect for a 1,3-substituted imidazo[5,1-*a*]isoquinoline relative to an imidazo[1,5-*a*]quinoline, as well as a good quantum yield of 38% at 473 nm.[10] Giordano described the synthesis of five imidazo[5,1-*a*]isoquinolines in 2023 and obtained quantum yields of up to 37% at 454 nm.[30] In our previous work, we reported the preparation and properties of several imidazo[1,5-*a*]quinolines **2** and imidazo[1,5-*a*]pyridines **3** that showed good emitter properties.[18–21]

So far, there have been great advances in the synthesis and functionalization of imidazo[1,2-*a*]pyridines,[31] imidazo[1,5-*a*]pyridines[17] and imidazo[1,5-*a*]quinolines.[21,32]

In this work, we investigate imidazo[5,1-a]isoquinolines **1** rather than imidazo[1,5-*a*]quinolines **2**. We study their absorption and emission behavior as well as quantum yields in solution, which were interpreted based on density functional theory (DFT) calculations. Cyclic voltammetry was used to analyze the effects of different substituents on the energy of the highest-occupied molecular orbital (HOMO).

Results and Discussion

In previous work, we have shown that imidazo[1,5-*a*]quinolines **2**, imidazo[1,5-*a*]pyridines **3** and an imidazo[5,1-*a*]isoquinoline **1** could be synthesized via an iodine-mediated condensation-cyclization-oxidation multi-step reaction (Scheme 1).[21,33] We now explore the applicability of this synthetic pathway for preparing new imidazo[5,1-*a*]isoquinolines **1** with different substituents in positions 1 and 3 (Scheme 1).

Imidazo[5,1-*a*]isoquinolines **1** could generally be obtained using this approach. The yield for **1 a** was initially unsatisfactory, although it can be significantly improved to 90% by extending the reaction time from 2–6 hours to two days (Scheme 2).

We prepared imidazoisoquinolines **1 a**–**1 h** (Figure 3) to study the influence of groups with different steric and electronic properties in position 3. In this first step, we used different substituents in position 3; a phenyl group was attached to position 1 in all compounds.

Using our optimized reaction conditions, we could obtain imidazo[5,1-*a*]isoquinolines **1 a**–**h** in good yields of up to 92% (Table 1) and characterize their photo- and electrochemical properties.

We prepared the corresponding imidazo[1,5-*a*]quinolines **2** with the same substituents in positions 1 and 3 to compare the new compounds' photo- and electrochemical properties (Ta-

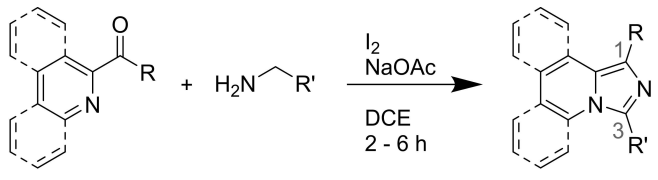

Scheme 1. The established synthetic pathway for creating imidazo[1,5-*a*]pyridines **3** and -quinolines **2**.

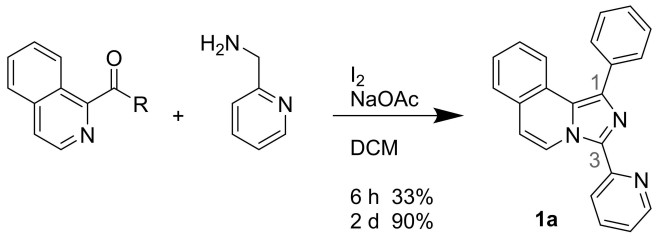

Scheme 2. Optimized conditions for the synthesis of **1 a**.

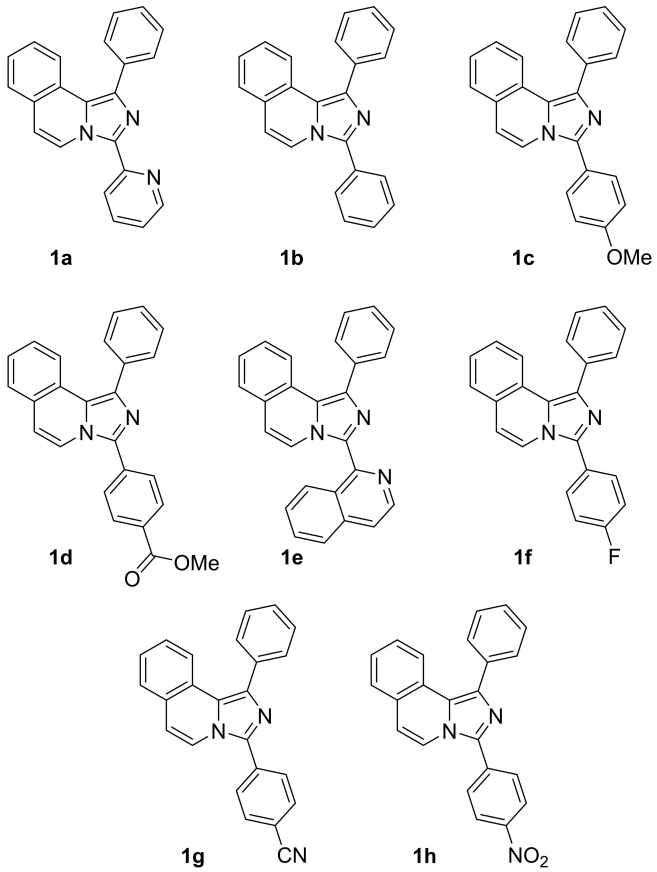

Figure 3. All imidazo[5,1-*a*]isoquinolines with different substituents in position 3.

Research Article
doi.org/10.1002/ejoc.202400298

Table 1. Molecules **1 a**–**h** and **2 a**–**h** with yield.

	R'	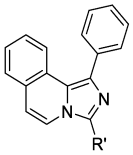	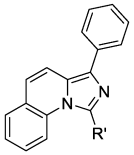
a		90 %	86 %
b		89 %	86 %
c	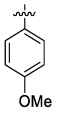	82 %	98 %
d	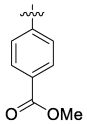	81 %	83 %
e		82 %	70 %
f	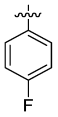	87 %	98 %
g	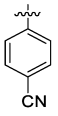	84 %	85 %
h	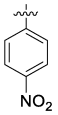	92 %	88 %

Table 2. Optical data of imidazo[5,1-*a*]isoquinolines **1 a**–**h** and imidazo[1,5-*a*]quinolines **2 a**–**h** measured in 0.1 mM chloroform solution.

	Extinction edge	Stokes shift	Extinction peak	Emission peak	Φ
1 a	406 nm	62 nm	369 nm	431 nm	33 %
2 a	424 nm	106 nm	356 nm	462 nm	14 %
1 b	390 nm	94 nm	335 nm	429 nm	7 %
2 b	418 nm	102 nm	362 nm	464 nm	34 %
1 c	394 nm	105 nm	336 nm	441 nm	5 %
2 c	420 nm	105 nm	364 nm	469 nm	25 %
1 d	414 nm	92 nm	359 nm	451 nm	36 %
2 d	430 nm	113 nm	362 nm	475 nm	14 %
1 e	434 nm	83 nm	381 nm	464 nm	31 %
2 e	428 nm	133 nm	358 nm	491 nm	14 %
1 f	388 nm	107 nm	335 nm	442 nm	5 %
2 f	414 nm	103 nm	363 nm	466 nm	32 %
1 g	412 nm	78 nm	368 nm	446 nm	48 %
2 g	428 nm	111 nm	363 nm	474 nm	19 %
1 h	484 nm	206 nm	412 nm	618 nm	< 1 %
2 h	502 nm	146 nm	428 nm	574 nm	< 1 %

ble 2). Among these, the synthesis of **1 a**,[34] **1 b**,[33,34] **2 a**[20] and **2 b**[35] have been reported in previous work.

Optical Measurements

Figure 4 shows the extinction and emission spectra of **1 a** and **2 a** and **1 b** and **2 b**. Tables and diagrams containing the extinction and emission data of **1 c**–**h** and **2 c**–**h** are attached in the SI (S2–S9). Changing the core from an imidazo[1,5-*a*]quinoline (**2 a**–**h**) to an imidazo[5,1-*a*]isoquinoline **1 a**–**h**, leads to a significant blue shift of 29.5 ± 5.5 nm, illustrating the hypsochromic effect of this molecular structure.

Comparison of the photoluminescence spectra for compounds with equal functional moieties shows that either imidazo[5,1-*a*]isoquinolines **1** or imidazo[1,5-*a*]quinolines **2** have the highest quantum yields, in dependence of the mesomeric effect of the substituents. Groups with a –M-effect

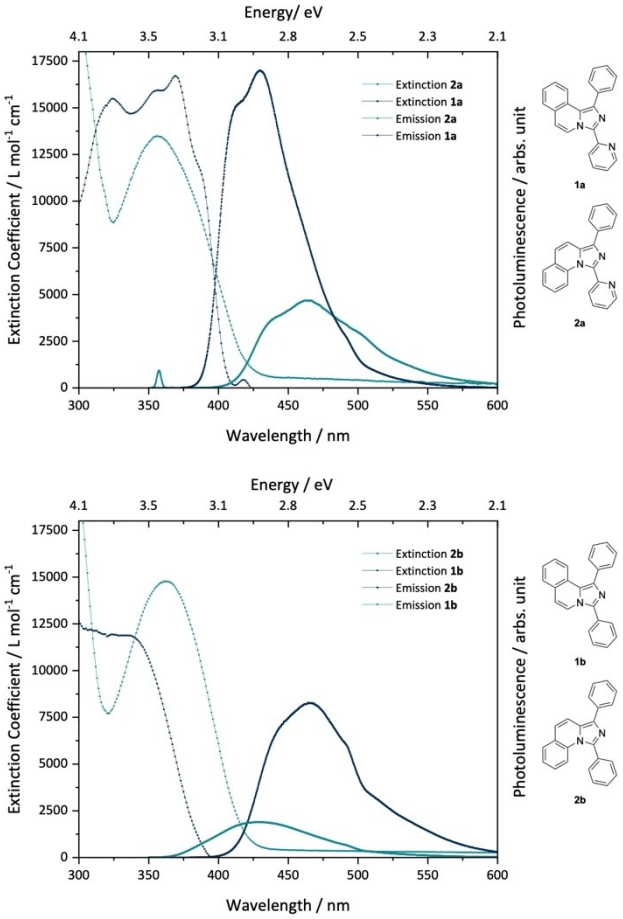

Figure 4. Top: Extinction and photoluminescence spectra of **1 a** and **2 a** in 0.1 mM chloroform. Bottom: Extinction and photoluminescence spectra of **1 b** and **2 b** in 0.1 mM chloroform.

in position 3 cause a higher quantum yield (Φ) in the imidazo[5,1-*a*]isoquinolines **1a**, **1d**, **1e**, and **1g** than their corresponding compounds **2a**, **2d**, **2e**, and **2g**.

Moieties with a +M-substituent in position 3 lead to a higher quantum yield (Φ) in **2b**, **2c**, and **2f** compared to **1b**, **1c**, and **1f**.

The highest quantum yield of all studied imidazo[1,5-*a*]quinolines was 34% for **2b**. The quantum yield increased to 48% for **1g**, which was the highest obtained for the new imidazo[5,1-*a*]isoquinolines. The quantum yield for **1h** and **2h** was very low, and the fluorescence was almost completely quenched.

The edge of extinction is observed at lower wavelengths for imidazo[5,1-*a*]isoquinolines **1a–h** than their corresponding compounds **2a–h**. This results in a significantly larger bandgap for all imidazo[5,1-*a*]isoquinolines except for **1e** compared to the homolog imidazo[1,5-*a*]quinoline **2e**. As this molecule has a sterically hindered group in position 3, we suppose this is due to steric reasons.

Again, **1h** and **2h** showed different behavior. They absorbed blue light and emitted red light. The quantum yield of both is very low, although they contain – with the nitro group – a –M-substituent. The bandgaps of **1h**, at 2.56 eV, and **2h**, at 2.47 eV, are much smaller than those of the other molecules.

Imidazo[1,5-*a*]quinolines **2a–h** showed Stokes shifts of 124 ± 22 nm, substantially larger than those of the imidazo[5,1-*a*]isoquinolines with 84.5 ± 22.5 nm. The imidazo[5,1-*a*]isoquinolines **1f** and **1h** were an exception; **1h** in particular had a Stokes shift of 206 nm compared to **2h**'s 146 nm.

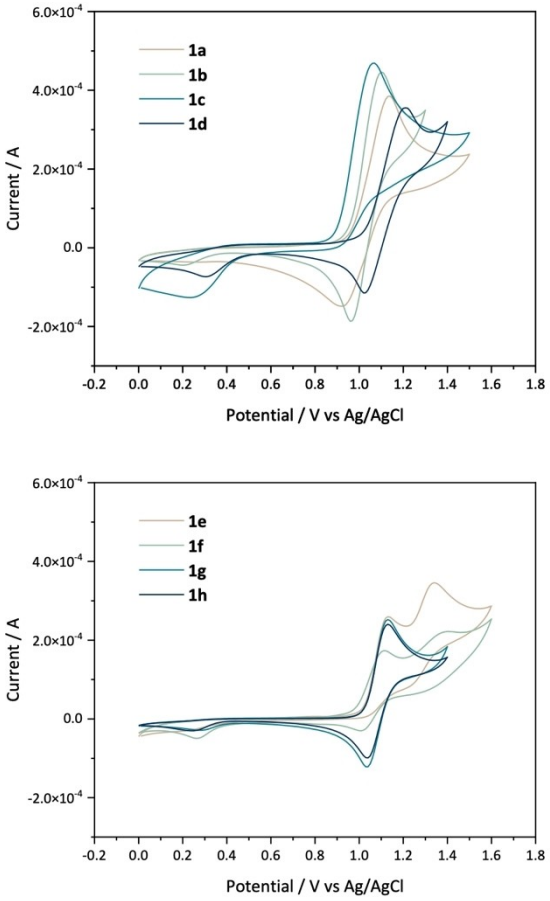

Figure 5. Top: Cyclic voltammograms of **1a–1d**. Bottom: Cyclic voltammograms of **1e–1h**. All were measured in 5 mM solutions in DMF with 0.1 M tetrabutylammoniumtetrafluoroborate at scan rates of 100 mVs^{-1}.

Structure and Energy Levels of Isolated Molecules

Figure 5 shows the cyclic voltammetry results for all imidazo[5,1-*a*]isoquinolines **1a–h** (those for **2a–h** are in the SI, as are the measurements with ferrocene as an internal standard; see SI chapter 3.1 and 3.2). The cyclic voltammograms show a clear oxidation peak for all samples.

All imidazo[5,1-*a*]isoquinolines except **1c**, **1e**, and **1f** showed a reversible oxidation in the cyclic voltammogram, as did the imidazo[1,5-*a*]pyridines **3** in our previous work.[20]

A second oxidation wave was observed for **2d**, **1–2e**, **1–2f**, **2g**, and **2h**, which could be ascribed to a second reversible oxidation. We observed similar behavior in previous studies of imidazo[1,5-*a*]quinolines **2**.[20]

No reductive signal upon scan reversal was obtained for **2a–h**, **1c**, **1e**, and **1f** at slower scanning rates. A small reduction signal could be detected by increasing the scan rate from 25 $mV{\cdot}s^{-1}$ to 500 $mV{\cdot}s^{-1}$ (see 3.1 and 3.2 in the SI). Previous measurements of other imidazo[1,5-*a*]quinolines[18] with different scan rates also showed a moderately fast chemical reaction that removed the oxidized molecules from the electrodes and, thereby, hindered the detection of their reduction at lower scan rates, an observation characteristic for such cases.[36] A subsequent slow irreversible process obviously follows the oxidation of the imidazo[1,5-*a*]quinolines **2** so that the direct reduction can only be observed using fast scan rates.[18,20]

Instead, or in addition, we found a reductive signal between 0.2 and 0.4 V in the voltammograms of all compounds except **1a**, **2a**, **2b**, **2e**, and **2g**. This signal was particularly large in those cases in which the direct reduction was suppressed. Therefore, we tentatively ascribe this signal to the reduction of the chemically modified oxidized species.

Due to the non-reversible character of the oxidation of all imidazo[1,5-*a*]quinolines **2** and the imidazo[5,1-*a*]isoquinolines **1c** and **1e**, this discussion is based on the values of the oxidation onset potential E^{Ox}_{onset}, the potential at which oxidation sets in. To discuss relative changes in ionization energy E_i, the onset potential was transformed and used to calculate energies based on how it related to the ionization energy $E_i \approx E_{HOMO} = -\left(4.6eV + 1.4 \cdot E^{ox}_{onset}\right)$.[37] Thus, E^{Ox}_{onset} from cyclic voltammetry, referred to as an internal ferrocene (Fc) standard, was used to calculate the HOMO energies (E_{HOMO}).[38] The LUMO energy E_{LUMO} was estimated by adding the energy E_{gap} obtained from the extinction gap.

In addition, we used DFT to calculate the values of HOMO and LUMO energies E^{DFT}_{HOMO} and E^{DFT}_{LUMO}, the values E^{DFT}_{gap} of the gap, and the local distribution of the orbitals for all molecules.

Research Article
doi.org/10.1002/ejoc.202400298

The trend of all calculated HOMO energies E_{HOMO}^{DFT} fits well with the values determined by cyclic voltammetry with a rather constant offset of 200 ± 190 meV between the calculated E_{HOMO}^{DFT} and the experimental electrochemical value E_{HOMO} (Table S1 with all the values is attached in the SI). A significant difference between the experimental and calculated values was found for the LUMO energy and, consequently, for the gap energy.[39] The experimental E_{LUMO} was found to be lower for the imidazo[1,5-*a*]quinolines **2a–g** than for the corresponding imidazo[5,1-*a*]isoquinolines **1a–g**. Similarly, the E_{gap} of 2.92 ± 0.06 eV for imidazo[1,5-*a*]quinolines **2a–g** was smaller than that of the corresponding imidazo[5,1-*a*]isoquinolines **1a–g**, which was 3.02 ± 0.16 eV. Both trends were confirmed by the calculated values of E_{LUMO}^{DFT} and E_{gap}^{DFT}.[39] A comparison of all gap energies (Figure 6) suggests a stronger stabilization of the electronically excited state in the imidazo[1,5-*a*]quinolines **2a–g** compared to the imidazo[5,1-*a*]isoquinolines **1a–g**, similar to previous results.[20] **1h** and **2h** show a much lower E_{LUMO} and much smaller E_{gap} than **1a–g** and **2a–g**.

Figure 7 shows the calculated orbitals for imidazo[5,1-*a*]isoquinolines **1a–h** (the DFT calculations of the imidazo[1,5-*a*]quinolines **2a–g** are shown in Figure S12 in the SI). The DFT calculations clearly show the HOMO density along the core and the moieties in position 1 and slightly less in position 3. Substituents in position 1 of imidazo[5,1-*a*]isoquinolines **1a–g** are not in plane with the core but are rotated a little out of plane. These substituents, therefore, probably have a reduced influence on the quantum yield and the spectroscopic properties of the molecules because of reduced conjugation with the aromatic system. In imidazo[1,5-*a*]quinolines **2a–g**, substituents in position 1 are in plane with the core, so these groups can enlarge the delocalized π-electron system for **2** compared to **1**.

Similar systematic trends were observed in the LUMO. For molecules with electron-withdrawing substituents in position 3, like **1–2a**, **1–2d**, **1–2e**, and **1–2g**, the substituents are in plane with the core and contribute to the LUMO considerably more than the core.

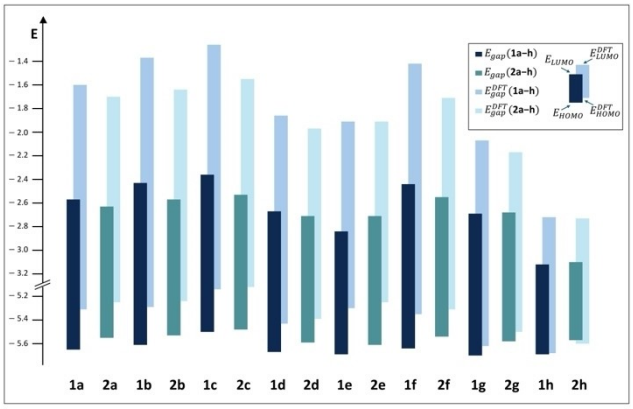

Figure 6. Electrochemically determined HOMO energy, optically determined energy gap and the derived LUMO energy, compared to the corresponding values calculated by DFT of all Imidazo[5,1-*a*]isoquinolines **1a-h** and Imidazo[1,5-*a*]quinolines **2a-h**.

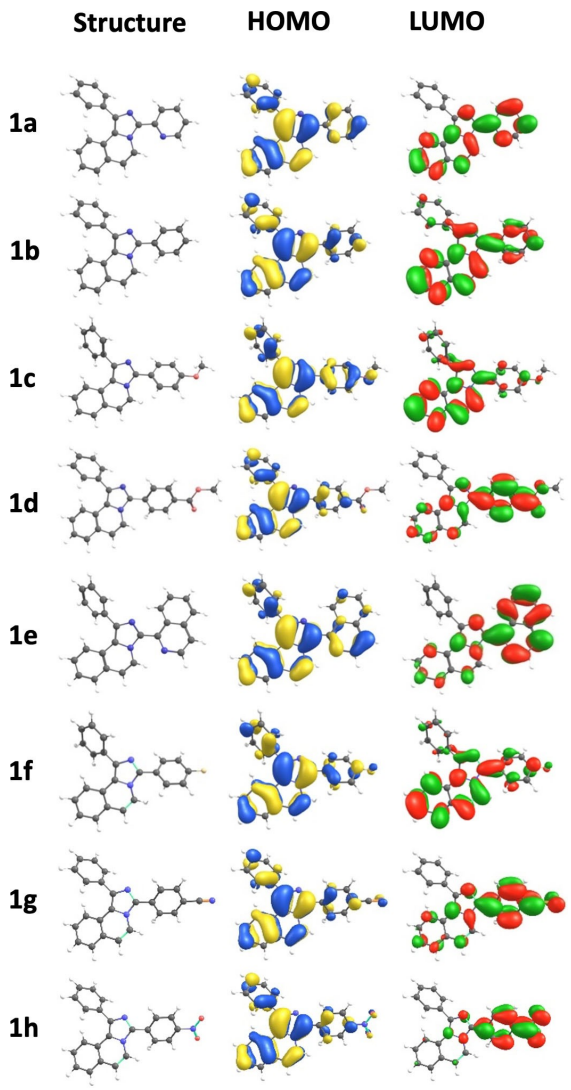

Figure 7. Calculated molecular structure and frontier orbitals of all imidazo[5,1-*a*]isoquinolines.

For **1–2b**, **1–2c**, and **1–2f**, the molecules with electron-donating substituents, these moieties are not in plane with the core and show almost no LUMO density compared to the molecules with –M-substituents. It is apparent that +M-substituents in position 3 do not substantially influence the quantum yield for imidazo[5,1-*a*]isoquinolines **1** but do for imidazo[1,5-*a*]quinolines **2**.

The DFT calculations for **1h** show a separation of HOMO and LUMO density. HOMO density is mainly in the core and position 1. There is little LUMO density in the core, but it is found in the rest of the structure and position 3. Such a small local overlap between HOMO and LUMO explains the low quantum yield despite a very strong –M-character of the 4-nitrophenyl group in position 3. The –M-effect is most likely too strong in this case.

A comparison of the calculated dipole moments (μ) of **1** and **2** (Table S1 attached in the SI) shows that molecules with a larger μ usually provide a higher quantum yield. Only for **1a**

Research Article
doi.org/10.1002/ejoc.202400298

compared to **2a** and **1e** compared to **2e** do we see a much smaller dipole moment but a higher quantum yield.

The observed hypsochromic shift in the absorption spectra may originate from reducing the effective size of the delocalized π-electron system. The fewer conjugated double bonds a system contains, the shorter the wavelength. A reduction in the size of the delocalized π-electron system in imidazo[5,1-*a*]isoquinolines **1** compared to imidazo[1,5-*a*]quinolines **2** can be concluded since we observed a systematic hypsochromic effect in **1** compared to **2**. This leads to the observed increase in the bandgap E_{gap} of 0.13 ± 0.09 eV for **1** compared to that of **2**. These values are very well confirmed through the DFT calculations by E_{gap}^{DFT} for **1**, which are larger by about 0.20 ± 0.14 eV than those for **2**.

The reduction in the size of the delocalized π-electron system is probably because the groups in positions 1 and 3 partially rotate out of plane in imidazo[5,1-*a*]isoquinolines **1**. In the case of imidazo[1,5-*a*]quinolines **2**, the phenyl group in position 1 is mostly in plane with the core, which results in an enlargement of the delocalized π-electron system.

The group in position 3 has a strong electronic effect, which could explain the differences in the observed quantum yields of the imidazo[5,1-*a*]isoquinolines **1**. These substituents are largely in plane and can, thus, have a stronger effect on the system than in the homologous imidazo[1,5-*a*]quinolines **2**, where the substituents rotate out of plane and can no longer interact effectively with the core π-system.

Conclusions

In this work, we synthesized a series of new imidazo[5,1-*a*]isoquinolines **1** in very good yields and the corresponding imidazo[1,5-*a*]quinolines **2** with the same substituents and compared their photo- and electrochemical properties.

The quantum yield was 48% for **1g**, which is the highest quantum yield reported for imidazo[5,1-*a*]isoquinolines. All imidazo[5,1-*a*]isoquinolines showed a clear hypsochromic effect.

The photochemical studies showed that moieties in position 3 greatly influence the quantum yield. If there is a −M-substituent in position 3, the quantum yield is very high for imidazo[5,1-*a*]isoquinolines and low for imidazo[1,5-*a*]quinolines. In the case of a +M-substituent in position 3, the quantum yield is high for imidazo[1,5-*a*]quinolines and lower for imidazo[5,1-*a*]isoquinolines.

Based on the observed systematic variation of emission wavelength and quantum efficiency, these new emitter molecules could, with tuning, be prospective candidates for blue OLEDs.

Experimental Section

All chemicals and solvents were purchased from commercial chemical suppliers. Each starting material was used without any further purification. All solvents were purified by distillation or were obtained from Acros in an AcroSeal bottle.

The reaction conditions for preparing the ketones have been reported earlier.[18,19]

For preparative column chromatography, Merck 9385 silica gel, pore size 60 Å (230-400 mesh), or an ARMEN Instrument SPOT liquid chromatography (medium-pressure liquid chromatography (MPLC)) system with GRACE Reverlis® flash cartridges (12 5.60 g, particle size 20 μm or 40 μm) was used.

NMR spectra were recorded on a Bruker Avance II 400 MHz or Avance III 600 MHz spectrometer in $CDCl_3$. All chemical shifts (δ) are reported in parts per million (ppm) and were referenced to the solvent residual peak ($\delta = 7.26$ or 77.16 ppm).[40] ^{13}C-NMR was recorded as phase-sensitive APT-spectra.

Multiplicity is indicated as s (singlet), d (duplet), dd (doublet of doublets), t (triplet), and m (multiplet); coupling constants (*J*) are expressed in Hz. High-resolution mass spectrometry (HRMS) was done on a Bruker MicroTOF to record mass spectra by electron-spray ionization (ESI).

Synthesis Method[33]

Ketone (0.25 mmol), amine (0.27 mmol), molecular iodine (0.3 mmol), and NaOAc (0.75 mmol) were dissolved in 15 mL dichloromethane (DCM) and heated at reflux for 2–6 h (**2a**–**h**) or for 2 days (**1a**–**h**). After cooling to room temperature, the reaction mixture was quenched with 5% $Na_2S_2O_3$ (2 mL) and H_2O (6 mL) and extracted three times with 10 mL dichloromethane (DCM). The combined organic layers were dried over Na_2SO_4, and the solvent was evaporated. The product was obtained after flash chromatography.

1-Phenyl-3-(2-pyridinyl)imidazo[5,1-*a*]isoquinoline 1a

Eluted with pentane:DCM:EtOAc (4.5:5.5:1.5). Yield: 496 mg (90%) rose solid, mp 210 °C. ^{1}H NMR ($CDCl_3$, 400 MHz): $\delta = 9.78$ (d, $J = 7.70$ Hz, 1H), 8.68 (d, $J = 4.53$ Hz, 1H), 8.45 (d, $J = 8.15$ Hz, 1H), 8.05 (d, $J = 8.15$ Hz, 1H), 7.82–7.74 (m, 3H), 7.60 (d, $J = 7.70$ Hz, 1H), 7.53 (t, $J = 7.25$ Hz, 2H), 7.50–7.44 (m, 1H), 7.42–7.36 (m, 1H), 7.34–7.22 (m, 2H), 6.93 (d, $J = 7.70$ Hz, 1H). ^{13}C NMR ($CDCl_3$, 151 MHz): $\delta =$ 150.8, 148.3, 136.9, 136.8, 136.3, 135.8, 130.1, 128.8, 128.2, 128.1, 127.7, 127.2, 127.0, 125.6, 125.3, 124.4, 123.2, 122.9, 122.5, 114.5. HRMS (ESI): $[M + H]^+$ calculated for $C_{22}H_{16}N_3^+$: 322.1339; found: 322.1341 $[M + Na]^+$ calculated for $C_{22}H_{15}N_3Na^+$: 344.1158; found: 344.1161. Anal. Calcd. for $C_{22}H_{15}N_3$: C, 82.22, H, 4.70, N, 13.08. Found: C, 81.99, H, 4.66, N, 13.01.

1-Phenyl-3-(2-pyridinyl)imidazo[1,5-*a*]quinoline 2a

Eluted with pentane:DCM:EtOAc (9:0.66:0.33). Yield: 294 mg (81%) yellow solid, mp 168 °C. ^{1}H NMR ($CDCl_3$, 600 MHz): $\delta = 8.75$ (ddd, $J =$ 4.8, 1.8, 0.9 Hz, 1H), 8.00 (dt, $J = 7.8$, 1.2 Hz, 1H), 7.97–7.88 (m, 3H), 7.70 (d, $J = 9.5$ Hz, 1H), 7.64 (dd, $J = 7.8$, 1.6 Hz, 1H), 7.53–7.46 (m, 3H), 7.91–7.40 (m, 1H), 7.40–7.30 (m, 2H), 7.25 (ddd, $J = 8.7$, 7.2, 1.6 Hz, 1H), 7.14 (d, $J = 9.4$ Hz, 1H). ^{13}C NMR ($CDCl_3$, 151 MHz): $\delta =$ 152.2, 149.5, 140.9, 137.5, 134.3, 134.2, 132.3, 129.0, 128.5, 127.7, 127.6, 127.5, 127.3, 125.9, 125.7, 124.1, 123.1, 118.5, 117.2. HRMS (ESI): $[M + H]^+$ calculated for $C_{22}H_{16}N_3^+$: 322.1339; found: 322.1338 and $[M + Na]^+$ calculated for $C_{22}H_{15}N_3Na^+$: 344.1158; found: 344.1157. Anal. Calcd. for $C_{22}H_{15}N_3$: C, 82.22, H, 4.70, N, 13.08. Found: C, 81.72, H, 4.50, N, 12.62.

1-Phenyl-3-(phenyl)imidazo[5,1-*a*]isoquinoline 1b

Eluted with pentane:DCM:EtOAc (4.5:5.5:1.5). Yield: 610 mg (89%) white solid, mp 174 °C. ^{1}H NMR ($CDCl_3$, 400 MHz): δ = 8.08 (d, J = 8.25 Hz, 1H), 8.00 (d, J = 7.54 Hz, 1H), 7.88–7.82 (m, 2H), 7.82–7.77 (m, 2H), 7.60–7.48 (m, 6H), 7.48–7.41 (m, 1H),7.38 (dt, J = 6.42 Hz, 1.22 Hz, 1H), 7.31 (dt, J = 8.15 Hz, 1.43 Hz, 1H), 6.81 (d, J = 7.54 Hz, 1H),. ^{13}C NMR ($CDCl_3$, 151 MHz): δ = 140.3, 130.0, 129.5, 129.2, 129.4, 128.8, 128.1, 127.8, 127.3, 127.1, 125.8, 124.2, 122.8, 120.8, 114.7. HRMS (ESI): $[M + Na]^+$ calculated for $C_{23}H_{16}N_2Na^+$: 343.1205; found: 343.1203. Anal. Calcd. for $C_{23}H_{16}N_2$: C, 86.22, H, 5.03, N, 8.74. Found: C, 85.92, H, 5.00, N, 8.53.

1-Phenyl-3-(phenyl)imidazo[1,5-*a*]quinoline 2b

Eluted with pentane:DCM:EtOAc (4.5:5.5:1.5). Yield: 38 mg (86%) yellow solid, mp 162 °C. ^{1}H NMR ($CDCl_3$, 400 MHz): δ = 7.96–7.90 (m, 2H), 7.74–7.66 (m, 3H), 7.63 (dd, J = 7.74 Hz, J = 1.15 Hz, 1H), 7.58–7.52 (m, 3H), 7.52–7.44 (m, 3H), 7.38–7.28 (m, 1H), 7.08 (d, J = 9.17 Hz, 1H). ^{13}C NMR ($CDCl_3$, 151 MHz): δ = 142.2, 132.6, 129.9, 129.6, 129.0, 128.8, 128.6, 127.6, 127.2, 126.6, 125.9, 125.4, 122.2, 117.7, 117.6. HRMS (ESI): $[M + H]^+$ calculated for $C_{23}H_{17}N_2^+$: 321.1386; found: 321.1389 and $[M + Na]^+$ calculated for $C_{23}H_{17}N_2Na^+$: 343.1205; found: 343.1203. Anal. Calcd. for $C_{23}H_{16}N_2$: C, 86.22, H, 5.03, N, 8.74. Found: C, 85.92, H, 4.95, N, 8.34.

3-(4-Methoxyphenyl)-1-(phenyl)imidazo[5,1-*a*]isoquinoline 1c

Eluted with pentane:DCM:EtOAc (4.5:5.5:1.5). Yield: 616 mg (82%) white solid, mp 184 °C. ^{1}H NMR ($CDCl_3$, 400 MHz): δ = 8.06 (d, J = 8.00 Hz, 1H), 7.93 (d, J = 7.50 Hz, 1H), 7.79 (d, J = 7.30 Hz, 2H), 7.75 (d, J = 8.60 Hz, 2H), 7.52 (dd, J = 14,79 Hz, 7.60 Hz, 3H), 7.42 (t, J = 7.30 Hz, 1H), 7.35 (t, J = 7.40 Hz, 1H), 7.32–7.28 (m, 1H), 7.06 (d, J = 8.84 Hz, 2H), 6.76 (d, J = 7.53 Hz, 1H), 3.89 (s, 3H),. ^{13}C NMR ($CDCl_3$, 151 MHz): δ = 141.3, 133.8, 130.9, 130.8, 130.1, 128.9, 128.6, 128.5, 127.8, 127.4, 127.2, 126.3, 123.8, 122.9, 122.7, 120.6, 114.7, 55.6. HRMS (ESI): $[M + H]^+$ calculated for $C_{24}H_{19}N_2O^+$: 351.1492; found: 351.1494. Anal. Calcd. for $C_{24}H_{18}N_2O$: C, 82.26, H, 5.18, N, 7.99. Found: C, 82.10, H, 4.91, N, 7.13.

3-(4-Methoxyphenyl)-1-(phenyl)imidazo[1,5-*a*]quinoline 2c

Eluted with pentane:DCM:EtOAc (4.5:5.5:1.5). Yield: 72 mg (98%) yellow solid, mp 184 °C. ^{1}H NMR ($CDCl_3$, 600 MHz): δ = 7.93 (d, J = 7.07 Hz, 2H), 7.67 (d, J = 9.32 Hz, 1H), 7.65–7.58 (m, 3H), 7.53 (d, J = 8.99 Hz, 1H), 7.48 (t, J = 7.39 Hz, 2H), 7.38–7.28 (m, 2H), 7.23–7.16 (m, 1H), 7.10–7.02 (m, 3H), 3.92 (s, 3H). ^{13}C NMR ($CDCl_3$, 151 MHz): δ = 160.7, 142.1, 134.3, 133.4, 132.7, 131.3, 131.1, 128.8, 128.6, 127.6, 127.1, 126.4, 125.9, 125.3, 125.1, 122.2, 117.6, 114.5. HRMS (ESI): $[M + H]^+$ calculated for $C_{24}H_{19}N_2O^+$: 351.1492; found: 351.1492. Anal. Calcd. for $C_{24}H_{18}N_2O$: C, 82.26, H, 5.18, N, 7.99. Found: C, 81.34, H, 5.16, N, 7.65.

3-(4-Methylacetat-phenyl)-1-(phenyl)imidazo[5,1-*a*]isoquinoline 1d

Eluted with pentane:DCM:EtOAc (4.5:5.5:1.5). Yield: 632 mg (81%) white solid, mp 224 °C. ^{1}H NMR ($CDCl_3$, 400 MHz): δ = 8.20 (d, J = 8.50 Hz, 2H), 8.06 (d, J = 7.89 Hz, 1H), 8.03 (d, J = 7.29 Hz, 1H), 7.94 (d, J = 8.50 Hz, 2H), 7.78 (d, J = 6.98 Hz, 2H), 7.57 (d, J = 7.59 Hz, 1H), 7.55–7.49 (m, 2H), 7.48–7.42 (m, 1H), 7.42–7.36 (m, 1H), 7.35–7.28 (m, 1H), 6.85 (d, J = 7.59 Hz, 1H), 3.96 (s, 3H). ^{13}C NMR ($CDCl_3$, 151 MHz): δ = 166.7, 139.1, 136.2, 134.1, 130.4, 130.3, 129.9, 128.8, 128.6, 128.3, 128.2, 127.8, 127.3, 125.7, 124.9, 122.9, 120.5, 114.9, 52.4. HRMS (ESI): $[M + H]^+$ calculated for $C_{25}H_{19}N_2O_2^+$: 379.1441; found: 349.1443. Anal. Calcd. for $C_{25}H_{19}N_2O_2$: C, 79.35, H, 4.79, N, 7.40. Found: C, 79.28, H, 4.59 N, 7.38.

3-(4-Methylacetat-phenyl)-1-(phenyl)imidazo[1,5-*a*]quinoline 2d

Eluted with pentane:DCM:EtOAc (4.5:5.5:1.5). Yield: 676 mg (83%) yellow solid, mp 186 °C. ^{1}H NMR ($CDCl_3$, 400 MHz): δ = 8.21 (d, J = 8.34 Hz, 2H), 7.89 (d, J = 7.25 Hz, 2H), 7.81 (d, J = 8.34 Hz, 2H), 7.69 (d, J = 9.43 Hz, 1H), 7.65 (d, J = 6.53 Hz, 1H), 7.51–7.44 (m, 3H), 7.35 (t, J = 7.50 Hz, 2H), 7.24–7.18 (m, 1H), 7.12 (d, J = 9.55 Hz, 1H), 3.99 (s, 3H). ^{13}C NMR ($CDCl_3$, 151 MHz): δ = 166.8, 141.1, 132.3, 130.9, 130.2, 129.9, 1298, 129.7, 129.1, 129.0, 128.9, 128.8, 128.6, 127.9, 127.8, 127.6, 127.4, 127.1, 126.9, 125.9, 125.7, 122.6, 117.7, 117.6, 52.5. HRMS (ESI): $[M + Na]^+$ calculated for $C_{25}H_{19}N_2O_2Na^+$: 401.1260; found: 401.1262. Anal. Calcd. for $C_{25}H_{19}N_2O_2$: C, 79.35, H, 4.79, N, 7.40. Found: C, 78.88, H, 4.71, N, 7.42.

3-(Isochinoyl)-1-(phenyl)imidazo[5,1-*a*]isoquinoline 1e

Eluted with pentane:DCM:EtOAc (4.5:5.5:1.5). Yield: 766 mg (94%) yellow solid, mp 162 °C. ^{1}H NMR ($CDCl_3$, 400 MHz): δ = 9.28 (d, J = 8.43 Hz, 1H), 9.00 (d, J = 7.59 Hz, 1H), 8.66 (d, J = 7.69 Hz, 1H), 8.16 (d, J = 8.01 Hz, 1H), 7.88 (d, J = 7.16 Hz, 3H), 7.76–7.64 (m, 3H), 7.62 (d, J = 7.59 Hz, 1H), 7.60–7.52 (m, 2H), 7.52–7.45 (m, 1H), 7.42 (dt, J = 6.74 Hz, 1.05 Hz, 1H), 7.33 (dt, J = 6.74 Hz, 1.26 Hz, 1H), 6.92 (d, J = 7.59 Hz, 1H). ^{13}C NMR ($CDCl_3$, 151 MHz): δ = 149.1, 141.1, 137.5, 136.9, 136.5, 135.8, 130.6, 130.1, 128.7, 128.6, 128.5, 128.4, 128.1, 127.8, 127.7, 127.3, 127.1, 126.9, 125.3, 125.2, 123.1, 1230, 121.2, 114.5. HRMS (ESI): $[M + Na]^+$ calculated for $C_{26}H_{17}N_3Na^+$: 394.1314; found: 394.1317. Anal. Calcd. for $C_{26}H_{17}N_3$: C, 84.07, H, 4.61, N, 11.31. Found: C, 83.94, H, 4.40, N, 11.11.

3-(Isochinoyl)-1-(phenyl)imidazo[1,5-*a*]quinoline 2e

Eluted with pentane:DCM:EtOAc (9:0.66:0.33). Yield: 276 mg (70%) yellow solid, mp 198 °C. ^{1}H NMR ($CDCl_3$, 400 MHz): δ = 8.78 (d, J = 5.50 Hz, 1H), 8.09 (d, J = 8.24 Hz, 1H), 8.02–7.94 (m, 3H), 7.88 (d, J = 5.86 Hz, 1H), 7.80 (d, J = 9.34 Hz, 1H), 7.77–7.72 (m, 1H), 7.63 (dd, J = 6.78 Hz 1.47 Hz, 2H), 7.60–7.53 (m, 1H), 7.53–7.46 (m, 2H), 7.38–7.32 (m, 1H), 7.30–7.22 (m, 1H), 7.18 (d, J = 9.53 Hz, 1H), 7.08–7.00 (m, 1H), 6.86 (d, J = 8.73 Hz, 1H). ^{13}C NMR ($CDCl_3$, 151 MHz): δ = 152.8, 142.5, 138.6, 137.1, 134.5, 134.1, 132.1, 130.9, 128.7, 128.5, 128.4, 127.9, 127.6, 127.3, 127.1, 127.0, 126.8, 125.6, 125.4, 122.9, 122.1, 117.6, 117.3. HRMS (ESI): $[M + Na]^+$ calculated for $C_{26}H_{17}N_3Na^+$: 394.1314; found: 394.1309. Anal. Calcd. for $C_{26}H_{17}N_3$: C, 84.07, H, 4.61, N, 11.31. Found: C, 83.47, H, 4.31, N, 11.11.

3-(4-Fluorophenyl)-1-(phenyl)imidazo[5,1-*a*]isoquinoline 1f

Eluted with pentane:DCM:EtOAc (4.5:5.5:1.5). Yield: 630 mg (87%) white solid, mp 198 °C. ^{1}H NMR ($CDCl_3$, 400 MHz): δ = 8.10 (d, J = 7.83 Hz, 1H), 7.94 (d, J = 7.83 Hz, 1H), 7.88–7.76 (m, 4H), 7.60–7.50 (m, 3H), 7.50–7.42 (m, 1H), 7.40 (dt, J = 7.15 Hz, 1.02 Hz,1H), 7.33 (m, 2H), 7.40 (dt, J = 7.15 Hz, 1.02 Hz,1H), 7.30–7.22 (m, 2H), 6.82 (d, J = 7.64 Hz, 1H). ^{13}C NMR ($CDCl_3$, 151 MHz): δ = 164.7, 162.2, 139.3, 131.1, 131.0, 129.9, 128.8, 128.3, 128.2, 127.7, 127.3, 127.2, 125.8, 124.2, 122.8, 120.5, 116.4, 116.2, 114.8. HRMS (ESI): $[M + H]^+$ calculated for $C_{23}H_{16}FN_2^+$: 339.1292; found: 339.1286 and $[M + Na]^+$ calculated for $C_{23}H_{15}FN_2Na^+$: 361.1111; found: 361.1110. Anal. Calcd. for $C_{23}H_{15}FN_2$: C, 81.64, H, 4.47, N, 8.28. Found: C, 81.15, H, 4.26, N, 8.26.

3-(4-Fluorophenyl)-1-(phenyl)imidazo[1,5-*a*]quinoline 2f

Eluted with pentane:DCM:EtOAc (4.5:5.5:1.5). Yield: 364 mg (98%) yellow solid, mp 198 °C. ^{1}H NMR ($CDCl_3$, 400 MHz): δ = 8.16 (d, J = 7.04 Hz, 1H), 7.96 (d, J = 7.04 Hz, 2H), 7.90–7.80 (m, 3H), 7.50 (t, J = 7.71 Hz, 2H), 7.34 (t, J = 7.37 Hz, 1H), 7.26 (t, J = 8.71 Hz, 2H), 6.86–6.78 (m, 1H), 6.64–6.58 (m, 2H). ^{13}C NMR ($CDCl_3$, 151 MHz): δ = 164.8, 162.4, 141.1, 134.3, 133.8, 132.5, 132.0, 131.9, 129.6, 129.0, 128.9, 128.8, 128.7, 127.7, 127.6, 127.5, 127.3, 126.6, 126.2, 125.9, 125.5, 122.4, 117.6, 117.4, 117.2, 116.5, 116.3, 116.1. HRMS (ESI): $[M + Na]^+$ calculated for $C_{23}H_{15}FN_2Na^+$: 361.1111; found: 361.1107. Anal. Calcd. for $C_{23}H_{15}FN_2$: C, 81.64, H, 4.47, N, 8.28. Found: C, 81.18, H, 4.32, N, 7.88.

3-(4-Cyanophenyl)-1-(phenyl)imidazo[5,1-*a*]isoquinoline 1g

Eluted with pentane:DCM:EtOAc (4.5:5.5:1.5). Yield: 548 mg (84%) yellow solid, mp 280 °C. ^{1}H NMR ($CDCl_3$, 600 MHz): δ = 8.07 (d, J = 8.02 Hz, 1H), 8.04–7.96 (m, 3H), 7.82 (d, J = 8.02 Hz, 2H), 7.76 (d, J = 7.38 Hz, 2H), 7.60 (d, J = 7.38 Hz, 2H), 7.56–7.50 (m, 2H), 7.50–7.46 (m, 1H), 7.46–7.38 (m, 1H), 7.38–7.30 (m, 1H). ^{13}C NMR ($CDCl_3$, 151 MHz): δ = 132.9, 129.9, 129.7, 129.1, 128.9, 128.6, 128.5, 127.8, 127.6, 127.4, 125.5, 125.3, 123.0, 120.0, 118.6, 115.8, 112.7. HRMS (ESI): $[M + Na]^+$ calculated for $C_{24}H_{15}N_3Na^+$: 368.1158; found: 368.1155. Anal. Calcd. for $C_{24}H_{15}N_3$: C, 83.46, H, 4.38, N, 12.17. Found: C, 83.13, H, 4.28, N, 12.10.

3-(4-Cyanophenyl)-1-(phenyl)imidazo[1,5-*a*]quinoline 2g

Eluted with pentane:DCM:EtOAc (4.5:5.5:1.5). Yield: 628 mg (85%) yellow solid, mp 240 °C. ^{1}H NMR ($CDCl_3$, 600 MHz): δ = 7.92–7.86 (m, 4H), 7.86–7.80 (m, 2H), 7.73–7.67 (m, 2H), 7.53–7.43 (m, 3H), 7.43–7.33 (m, 2H), 7.30–7.24 (m, 1H), 7.17 (d, J = 9.62 Hz, 1H). ^{13}C NMR ($CDCl_3$, 151 MHz): δ = 140.0, 137.9, 135.0, 134.1, 132.7, 132.1, 130.4, 129.0, 129.0, 127.9, 127.5, 127.5, 126.0, 126.0, 123.0, 118.6, 117.6, 117.5, 113.0. HRMS (ESI): $[M + Na]^+$ calculated for $C_{24}H_{15}N_3Na^+$: 368.1158; found: 368.1157. Anal. Calcd. for $C_{24}H_{15}N_3$: C, 83.46, H, 4.38, N, 12.17. Found: C, 83.06, H, 4.26, N, 11.67.

3-(4-Nitrophenyl)-1-(phenyl)imidazo[5,1-*a*]isoquinoline 1h

Eluted with pentane:DCM:EtOAc (4.5:5.5:1.5). Yield: 86 mg (92%) red solid, mp 226 °C. ^{1}H NMR ($CDCl_3$, 400 MHz): δ = 8.38 (d, J = 9.05 Hz, 2H), 8.10–8.02 (m, 4H), 7.76 (d, J = 7.10 Hz, 2H), 7.61 (d, J = 7.63 Hz, 1H), 7.58–7.50 (m, 2H), 7.50–7.39 (m, 2H), 7.38–7.30 (m, 1H), 6.92 (d, J = 7.63 Hz, 1H). ^{13}C NMR ($CDCl_3$, 151 MHz): δ = 147.7, 137.7, 136.7, 135.9, 135.6, 129.9, 129.1, 128.9, 128.6, 128.4, 127.8, 127.6, 127.4, 125.6, 125.5, 124.4, 123.0, 120.1, 115.7. HRMS (ESI): $[M + H]^+$ calculated for $C_{23}H_{16}N_3O_2^+$: 366.1237; found: 366.1238 and $[M + Na]^+$ calculated for $C_{23}H_{15}N_3O_2Na^+$: 388.1056; found: 388.1058. Anal. Calcd. for $C_{23}H_{15}N_3O_2$: C, 75.60, H, 4.14, N, 11.50. Found: C, 75.18, H, 3.97, N, 11.53.

3-(4-Nitrophenyl)-1-(phenyl)imidazo[1,5-*a*]quinoline 2h

Eluted with pentane:DCM:EtOAc (4.5:5.5:1.5). Yield: 342 mg (88%) red solid, mp 282 °C. ^{1}H NMR ($CDCl_3$, 600 MHz): δ = 8.40 (d, J = 8.57 Hz, 2H), 7.95 (d, J = 8.57 Hz, 2H), 7.90 (d, J = 7.08 Hz, 2H), 7.76–7.68 (m, 2H), 7.54–7.46 (m, 3H), 7.46–7.34 (m, 2H), 7.34–7.24 (m, 1H), 7.19 (d, J = 8.57 Hz, 1H). ^{13}C NMR ($CDCl_3$, 151 MHz): δ = 148.2, 139.7, 139.6, 132.0, 130.6, 129.1, 129.0, 128.0, 127.7, 126.1, 126.0, 124.2, 123.2, 117.7, 117.5. HRMS (ESI): $[M + H]^+$ calculated for $C_{23}H_{16}N_3O_2^+$: 366.1237; found: 366.1236 and $[M + Na]^+$ calculated for $C_{23}H_{15}N_3O_2Na^+$: 388.1056; found: 388.1057. Anal. Calcd. for $C_{23}H_{15}N_3O_2$: C, 75.60, H, 4.14, N, 11.50. Found: C, 75.51, H, 3.95, N, 11.33.

Optical Measurements

UV-vis extinction was measured with a Jena Specord 200 spectrometer for 0.1 mM solutions in $CHCl_3$ (n = 1.339).[41] The corresponding emission properties were obtained with a Jasco Germany FP 8300 spectrometer. An equally concentrated solution of quinine sulfate in 0.5 M H_2SO_4 (Φ = 0.546 and refractive index n = 1.445) was used as a reference for calculating the fluorescence quantum yield (Φ) of all molecules.[42][43] Φ was calculated as described in the literature.[44] The optical gap between the frontier orbitals of all substances was obtained by a linear fit of the extinction edge (see SI S1) and conversion of the intersection wavelength into an energy value (Formula 1).[39]

$$E_{gap} = h\frac{c}{\lambda}. \quad (1)$$

Electrochemical Measurements

Cyclic voltammetry was measured with an Ivium Technologies IviumStat potentiostat in a water-free (< 0.5 ppm) nitrogen atmosphere. 0.1 M tetrabutylammonium tetrafluoroborate (Sigma Aldrich) was added to a 5 mM solution of the substances in dimethylformamide (Carl Roth GmbH) as a supporting electrolyte. A standard three-electrode cell configuration was used with platinum wires as working and counter electrodes and a leak-free Ag/AgCl-electrode (LF-2, Warner Instruments) as a reference electrode. Ferrocene was used as an internal reference.[36] The discussion is based on values of E^{ox}_{onset}, determined by taking the first derivative of the current and linearly fitting the slope because of the irreversible characteristics of imidazo[1,5-*a*]quinoline and some imidazo[5,1-*a*]isoquinoline derivatives.[37] Using ferrocene as an internal standard allows the onset to be used to estimate the energy of the highest occupied molecular orbital (HOMO) (Formula 2).[38]

$$E_{HOMO} = -\left(4.6eV + 1.4 \cdot E^{ox}_{onset}\right). \quad (2)$$

DFT Calculations

All density functional theory computations were carried out using the Orca 5.0.3 program package. For structural optimizations and the acquisition of HOMO and LUMO energies, the B3LYP hybrid functional[45,46,47] with the Karlsruhe basis set def2-TZVP[48] was deployed. Structural minima were determined via conformational analysis with the Crest program[49] package and the absence of imaginary vibrational frequencies. The D3 scheme[50] with Becke-Johnson dampening[51,52] was used to account for dispersion interactions. The reader is referred to the SI for optimized compound geometries.

Acknowledgements

Open Access funding enabled and organized by Projekt DEAL.

Conflict of Interests

The authors declare no conflict of interest.

Data Availability Statement

The data that support the findings of this study are available in the supplementary material of this article.

Keywords: Imidazo[5,1-*a*]isoquinoline · Imidazo[1,5-*a*]quinoline · Heterocycles · Fluorescence

[1] D. Kim, L. Wang, J. J. Hale, C. L. Lynch, R. J. Budhu, M. Maccoss, S. G. Mills, L. Malkowitz, S. L. Gould, J. A. DeMartino, et al., *Bioorg. Med. Chem. Lett.* **2005**, *15*, 2129–2134.
[2] N. F. Ford, L. J. Browne, T. Campbell, C. Gemenden, R. Goldstein, C. Gude, J. W. Wasley, *J. Med. Chem.* **1985**, *28*, 164–170.
[3] L. J. Browne, C. Gude, H. Rodriguez, R. E. Steele, A. Bhatnager, *J. Med. Chem.* **1991**, *34*, 725–736.
[4] D. Davey, P. W. Erhardt, W. C. Lumma, J. Wiggins, M. Sullivan, D. Pang, E. Cantor, *J. Med. Chem.* **1987**, *30*, 1337–1342.
[5] R. Nirogi, A. R. Mohammed, A. K. Shinde, N. Bogaraju, S. R. Gagginapalli, S. R. Ravella, L. Kota, G. Bhyrapuneni, N. R. Muddana, V. Benade, et al., *Eur. J. Med. Chem.* **2015**, *103*, 289–301.
[6] D. J. Sanger, *Behav. Pharmacol.* **1995**, *6*, 116–126.
[7] H. Mikashima, K. Goto, *Yakugaku zasshi : Journal of the Pharmaceutical Society of Japan* **1982**, *102*, 99–103.
[8] H. Sheng, Y. Hu, Y. Zhou, S. Fan, Y. Cao, X. Zhao, W. Yang, *Dyes Pigm.* **2019**, *160*, 48–57.
[9] G. Albrecht, C. Geis, J. M. Herr, J. Ruhl, R. Göttlich, D. Schlettwein, *Org. Electron.* **2019**, *65*, 321–326.
[10] G. Volpi, B. Lace, C. Garino, E. Priola, E. Artuso, P. Cerreia Vioglio, C. Barolo, A. Fin, A. Genre, C. Prandi, *Dyes Pigm.* **2018**, *157*, 298–304.
[11] C. W. Tang, S. A. VanSlyke, *Appl. Phys. Lett.* **1987**, *51*, 913–915.
[12] S. Haneder, E. Da Como, J. Feldmann, J. M. Lupton, C. Lennartz, P. Erk, E. Fuchs, O. Molt, I. Münster, C. Schildknecht, et al., *Adv. Mater.* **2008**, *20*, 3325–3330.
[13] N. Thejo Kalyani, S. J. Dhoble, *Renewable Sustainable Energy Rev.* **2012**, *16*, 2696–2723.
[14] A. Marchesi, S. Brenna, G. A. Ardizzoia, *Dyes Pigm.* **2019**, *161*, 457–463.
[15] G. Volpi, G. Magnano, I. Benesperi, D. Saccone, E. Priola, V. Gianotti, M. Milanesio, E. Conterosito, C. Barolo, G. Viscardi, *Dyes Pigm.* **2017**, *137*, 152–164.
[16] K. Winterfeld, H. Franzke, *Angew. Chem. Int. Ed.* **1963**, *2*, 736–737.
[17] G. Volpi, *Asian J. Org. Chem.* **2022**, *11*, e202200171.
[18] G. Albrecht, J. M. Herr, M. Steinbach, H. Yanagi, R. Göttlich, D. Schlettwein, *Dyes Pigm.* **2018**, *158*, 334–341.
[19] J. M. Herr, C. Rössiger, G. Albrecht, H. Yanagi, R. Göttlich, *Synthesis* **2019**, 2931–2940.
[20] G. Albrecht, C. Rössiger, J. M. Herr, H. Locke, H. Yanagi, R. Göttlich, D. Schlettwein, *Phys. Status Solidi B* **2020**, *257*, 1900677.
[21] J. M. Herr, C. Rössiger, H. Locke, M. Wilhelm, J. Becker, W. Heimbrodt, D. Schlettwein, R. Göttlich, *Dyes Pigm.* **2020**, *180*, 108512.
[22] G. Volpi, C. Garino, L. Salassa, J. Fiedler, K. I. Hardcastle, R. Gobetto, C. Nervi, *Chem. Eur. J.* **2009**, *15*, 6415–6427.
[23] H. Zimmer, D. G. Glasgow, M. McClanahan, T. Novinson, *Tetrahedron Lett.* **1968**, 2805–2807.
[24] H. Reimlinger, J. J. M. Vandewalle, W. R. F. Lingier, E. de Ruiter, *Chem. Ber.* **1975**, *108*, 3771–3779.
[25] I. Yavari, G. Khalili, A. Mirzaei, *Helv. Chim. Acta* **2010**, *93*, 72–76.
[26] K. C. Langry, *J. Org. Chem.* **1991**, 2400–2404.
[27] J. Bori, N. Behera, S. Mahata, V. Manivannan, *ChemistrySelect* **2017**, *2*, 11727–11731.
[28] J. Bori, V. Manivannan, *J. Heterocycl. Chem.* **2022**, *59*, 1073–1078.
[29] G. Pelletier, A. B. Charette, *Org. Lett.* **2013**, *15*, 2290–2293.
[30] M. Giordano, G. Volpi, C. Garino, F. Cardano, C. Barolo, G. Viscardi, A. Fin, *Dyes Pigm.* **2023**, *218*, 111482.
[31] C.-H. Ma, M. Chen, Z.-W. Feng, Y. Zhang, J. Wang, Y.-Q. Jiang, B. Yu, *New J. Chem.* **2021**, *45*, 9302–9314.
[32] N. Kulhanek, N. Martin, R. Göttlich, *Eur. J. Org. Chem.* **2024**, *27*, e202301007.
[33] Z. Hu, J. Hou, J. Liu, W. Yu, J. Chang, *Org. Biomol. Chem.* **2018**, *16*, 5653–5660.
[34] M. E. Bluhm, M. Ciesielski, H. Görls, M. Döring, *Angew. Chem. Int. Ed.* **2002**, *41*, 2962–2965.
[35] a) H. Wang, W. Xu, Z. Wang, L. Yu, K. Xu, *J. Org. Chem.* **2015**, *80*, 2431–2435; b) G. Wang, J. Jia, G. Liu, M. Yu, X. Chu, X. Liu, X. Zhao, *Chem. Commun.* **2021**, *57*, 11811–11814; c) S. Chandrasekar, S. Sangeetha, G. Sekar, *ChemistrySelect* **2019**, *4*, 5651–5655; d) Y. Liao, C. Yan, R. Zhang, M. Cai, *J. Organomet. Chem.* **2019**, *881*, 1–12; e) M. Sandeep, P. Swati Dushyant, B. Sravani, K. Rajender Reddy, *Eur. J. Org. Chem.* **2018**, *2018*, 3036–3047.
[36] N. Elgrishi, K. J. Rountree, B. D. McCarthy, E. S. Rountree, T. T. Eisenhart, J. L. Dempsey, *J. Chem. Educ.* **2018**, *95*, 197–206.
[37] B. D'Andrade, S. Datta, S. Forrest, P. Djurovich, E. Polikarpov, M. Thompson, *Org. Electron.* **2005**, *6*, 11–20.
[38] J. Pommerehne, H. Vestweber, W. Guss, R. F. Mahrt, H. Bässler, M. Porsch, J. Daub, *Adv. Mater.* **1995**, *7*, 551–554.
[39] J. C. Costa, R. J. Taveira, C. F. Lima, A. Mendes, L. M. Santos, *Opt. Mater.* **2016**, *58*, 51–60.
[40] G. R. Fulmer, A. J. M. Miller, N. H. Sherden, H. E. Gottlieb, A. Nudelman, B. M. Stoltz, J. E. Bercaw, K. I. Goldberg, *Organometallics* **2010**, *29*, 2176–2179.
[41] S. Kendenburg, M. Vieweg, T. Gissibl, H. Giessen, *Opt. Mater. Express* **2012**, 1588–1611.
[42] D. F. Eaton in *Pure Appl. Chem.*, **1988**, *60*, 1107–1114.
[43] W. H. Melhuish, *J. Phys. Chem.* **1961**, 229–235.
[44] A. M. Brouwer, *Pure Appl. Chem.* **2011**, *83*, 2213–2228.
[45] C. Lee, W. Yang, R. G. Parr, *Phys. Rev. B* **1988**, *37*, 785–789.
[46] P. J. Stephens, F. J. Devlin, C. F. Chabalowski, M. J. Frisch, *J. Phys. Chem.* **1994**, 11623–11627.
[47] A. D. Becke, *J. Chem. Phys.* **1993**, *98*, 5648–5652.
[48] A. Schäfer, C. Huber, R. Ahlrichs, *J. Chem. Phys.* **1994**, *100*, 5829–5835.
[49] P. Pracht, F. Bohle, S. Grimme, *Phys. Chem. Chem. Phys.* **2020**, *22*, 7169–7192.
[50] S. Grimme, J. Antony, S. Ehrlich, H. Krieg, *J. Chem. Phys.* **2010**, *132*, 154104.
[51] E. R. Johnson, A. D. Becke, *J. Chem. Phys.* **2006**, *124*, 174104.
[52] A. D. Becke, E. R. Johnson, *J. Chem. Phys.* **2005**, *123*, 154101.

Manuscript received: March 19, 2024
Revised manuscript received: April 28, 2024
Accepted manuscript online: April 29, 2024
Version of record online: June 19, 2024